ISSN 2007-9737

Study of the Electric Field Distribution and Impedance Change in a 2D Multilayer Skin Model Using Interdigitated Electrodes

Daniela Campo[1], René Antaño-López[1], José Herrera-Celis[2,*]

[1] Centro de Investigación y Desarrollo Tecnológico en Electroquímica, Mexico

[2] Universidad Industrial de Santander, Colombia

dcampo@cideteq.mx, jherrece@uis.edu.co

Abstract. The skin's response to electrical stimuli depends not only on the composition and thickness of each layer but also on the geometry associated with the excitation electrodes. Therefore, an evaluation of the effects of electrode geometry is necessary. This study used the COMSOL Multiphysics® platform and a 2D model based on a simplified array of interdigitated electrodes connected to the skin. The skin was modeled as a multilayer structure representing the stratum corneum, epidermis, dermis, and subcutaneous tissue. This study analyzed how varying the distance between electrodes (100 µm to 10 mm) affects the electric field distribution and sensitivity to impedance changes after modifying the conductivity of the different skin layers. The optimal distance that maximizes sensitivity to these variations was identified, both in the presence and absence of the stratum corneum. In the presence of the stratum corneum, the maximum change in impedance due to variations in epidermal conductivity was found at an electrode distance of 2.1 mm. In contrast, no maxima were reported for variations in the conductivities of the dermis and subcutaneous tissue. In the absence of the stratum corneum, changes in the electrical conductivities of the epidermis, dermis, and subcutaneous tissue resulted in more significant impedance changes when the electrodes were spaced at 100 µm, 6.6 mm, and 9.1 mm, respectively. These results provide new opportunities for the non-invasive study of skin layers, which contain medically relevant information for drug delivery and disease monitoring using interdigitated electrodes.

Keywords. Bioimpedance, skin, interdigitated electrodes, finite element method, multilayer model.

1 Introduction

The complexity of the skin's multilayer structure makes it challenging to precisely and non-invasively characterize each layer, which may contain medically helpful information for various applications, such as drug delivery or the assessment of diseases like skin cancer, cardiovascular risk, obesity, and diabetes mellitus, among others [1].

Previous studies indicate that the frequency and distance between electrodes influence the depth of bioimpedance measurements [1–3]. Increasing the size and distance between electrodes can reduce the influence of the stratum corneum and facilitate measurements [1].

However, it can also cause currents to flow through deeper tissues, compromising the accuracy of assessing each layer of the skin. While the underlying tissues may dominate the measurements at high frequencies, detectable features at low frequencies remain hidden.

Furthermore, one must keep in mind that the relationship between measurement depth and frequency also depends on each individual's electrical and physiological parameters [1]. No specific electrode distance or frequency that maximizes the sensitivity of bioimpedance measurements on a particular skin layer has been determined yet.

Considering the limitations mentioned above, interdigitated electrodes (IDEs) are a good option

ISSN 2007-9737

for accessing and extracting information from specific layers of the skin. IDEs consist of a pair of planar electrodes arranged alternately, with dimensions that can be adjusted to control the depth of the applied electric field [4]. These electrodes would facilitate the characterization of one skin layer by concentrating the applied energy in a region of interest, thus minimizing the influence of adjacent layers.

The primary aim of this research was to analyze how variations in the geometric parameters of an interdigitated electrode array influence the electric field distribution and the sensitivity of impedance measurements to changes in the conductivity of specific skin layers.

Additionally, the study aimed to identify the electrode distance that maximizes sensitivity to these variations, both in the presence and absence of the stratum corneum.

2 Methodology

A 2D finite element model representing the multilayer structure of the skin was developed (see Fig. 1). This model includes the stratum corneum, epidermis, dermis, and subcutaneous tissue. Muscle was added as the bottom layer to give the model the appropriate depth relative to the electrode distance. The thicknesses and electrical properties of the different layers are shown in Table 1. Constant values for electrical properties were used across the entire frequency range.

Thanks to their symmetry, the IDEs can be simplified as only a pair of planar electrodes, where one is polarized and the other acts as ground. This simplification is valid if a specific geometric ratio between the electrode width and the distance between them is maintained [5]. In this case, the electrode width was half the distance between them (w/2).

The simulations were performed in COMSOL Multiphysics® 5.6, using the Electric Currents physics interface from the AC/DC Module. As boundary conditions, a potential of 1 V was applied between the electrodes, and electrical insulation was imposed on the outer boundaries of the model.

Table 1. Thickness (t), electrical conductivity (σ) and relative permittivity (ε_r) of the different skin layers considered in the 2D model

Layer	t [mm]	σ [S/m]	ε_r
Stratum corneum [a]	0.02	0.0005	2.4
Epidermis [a]	0.15	0.026	1
Dermis [a]	1	0.227	3.4
Subcutaneous tissue [a]	2	0.004	5.6
Muscle [b]	8	0.35182	10094

[a]Conductivities and relative permittivities from [6].
[b]Conductivity and relative permittivity from [7].

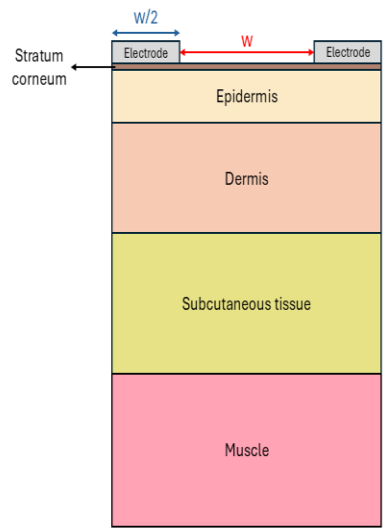

Fig. 1. Schematic diagram of the layers in the developed 2D model

Finally, a physics-controlled mesh with an extra fine element size was generated. To evaluate the effect of electrode distance on the sensitivity of bioimpedance measurements, an initial frequency domain study was conducted from 10 Hz to 1 MHz, with a parametric sweep of electrode distances from 100 μm to 10 mm. T

he system's total impedance and the average magnitude of the electric field in each skin layer were computed for each electrode distance. Additionally, the variation in impedance at 10 Hz was evaluated after increasing the conductivity of specific layers by an order of magnitude while maintaining the same range of electrode distances.

3 Results and Discussion

Fig. 2 shows the Nyquist plots obtained for electrode distances ranging from 1 to 10 mm, considering only the impedance of the simplified arrangement described in the previous section (see Fig. 1) and not including the total impedance of the IDEs.

As the distance between electrodes increases, the electrical impedance decreases in their real and imaginary parts. This is due to the contribution of deeper layers with higher electrical conductivity.

Based on the obtained spectra, it was determined that impedance variability would be analyzed at a frequency of 10 Hz, as more evident differences in impedance magnitude were observed at this value when varying the distances between electrodes.

Moreover, although increasing the frequency allows for the analysis of deeper layers, it may overlook relevant information obtained at lower frequencies, which is related to changes in the medium's conductivity. This presents an opportunity for more detailed analysis.

The electric field distribution across the different skin layers showed significant differences depending on the distance between electrodes but not for frequency. This is because, within the evaluated frequency range, no capacitive behavior significantly altering the impedance of each layer was observed, consequently preventing changes in the electric field distribution.

Fig. 3 shows the average magnitude of the electric field in the dermis for each electrode distance evaluated. As the distance between the electrodes increases, the electric field redistributes towards deeper layers, reaching a maximum in the dermis at 4.3 mm before decreasing as it disperses into lower layers.

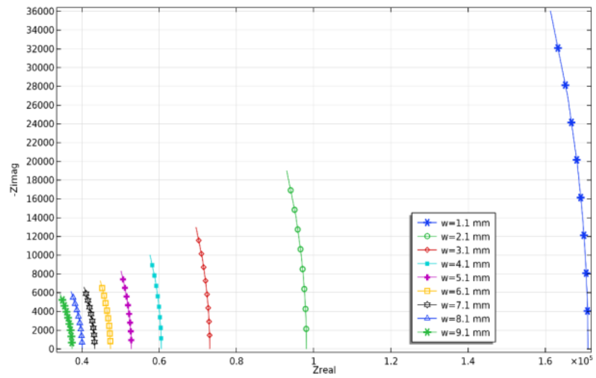

Fig. 2. Nyquist plots obtained for electrode distances ranging from 1 to 10 mm

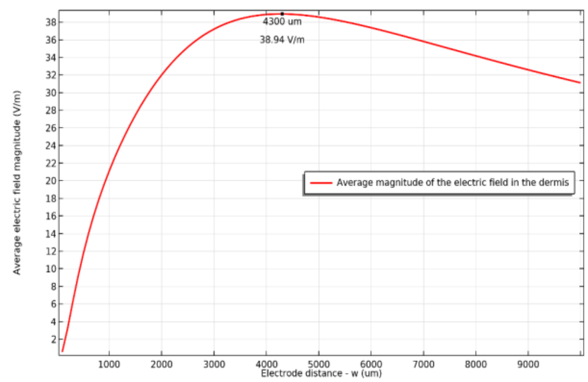

Fig. 3. Average magnitude of the electric field in the dermis for electrode distances ranging from 100 µm to 10 mm

Table 2 shows the distances at which the maximum average electric field was found in the epidermis, dermis, and hypodermis. This analysis was also performed on a model without the stratum corneum, so the corresponding maxima are included in the same table. Additionally, Table 2 presents the distance at which the most significant variation in electrical impedance was observed after increasing the conductivity of each layer, as well as the maximum impedance percentage variation obtained in each case.

The distance at which the maximum average electric field was observed does not coincide with the distance at which the most significant variation in electrical impedance was obtained in the different layers. This is because varying the electrical conductivity of a specific layer also

Table 2. Electrode distances at which the maximum average electric field (d_E) and impedance variation (d_Z) occur, together with their percentage change (ΔZ%), for each skin layer

Skin layer	With stratum corneum			Without stratum corneum		
	d_E	d_Z	ΔZ%	d_E	d_Z	ΔZ%
Epidermis	350 μm	2.1 mm	11.25 %	--	100 μm	89.86 %
Dermis	4.3 mm	--	--	1.6 mm	6.6 mm	66.23 %
Subcutaneous tissue	--	--	--	5.4 mm	9.1 mm	51.27%

alters the distribution of the electric field throughout the model, generating new maxima.

Additionally, the total measured impedance includes contributions from all layers, so even if the electric field is at its maximum in one layer at a certain distance, contributions from the other layers are not excluded.

Although these two variables are not correlated, identifying an electrode distance that maximizes the electric field in a specific skin layer could be particularly useful in techniques such as reverse iontophoresis. This technique involves extracting biomarkers from the skin by applying an electric current [8]. Using IDEs would allow for the efficient extraction of biomarkers from the layer where they are produced by maximizing the electric field in that region.

The most significant variation in electrical impedance observed at a specific electrode distance is probable because, at that distance, more current flows through the layer of interest, resulting in a more significant percentage change in impedance when the conductivity of that layer increases. In cases where no maximum was detected, it is necessary to evaluate greater distances between the electrodes to identify it.

The stratum corneum can be removed through methods such as moisturization-tape stripping or microdermabrasion (exfoliation) [9], [10]. According to the results, removing the stratum corneum results in impedance measurements that exhibit increased sensitivity to changes in the deeper layers of the skin with a shorter electrode distance. This is due to the removal of a highly resistive layer where most of the electric field is concentrated, allowing the field to redistribute in the lower layers and increasing the sensitivity of the measurement to changes in these layers.

This work does not consider the effects of the electrical double layer present at the electrode-skin interface. Incorporating it into the model would increase the magnitude of the measured impedance, especially at low frequencies. However, this phenomenon would not affect the electrode distances at which the maxima of the electric field and impedance variation are found.

4 Conclusions

The electrode distances for maximizing the sensitivity of impedance measurements to changes in skin layer electrical conductivities were identified in the presence and absence of the stratum corneum. These results represent an initial step toward the non-invasive exploration of different skin layers through electrical bioimpedance measurements using IDEs, thus facilitating the acquisition of clinically relevant information.

In the same way, the electrode distances at which the average electric field in each skin layer reaches its maximum were identified. These results can be applied for non-invasive extraction of biomarkers produced in specific skin layers.

In future work, simulations that consider the electrode-skin interface phenomenon are proposed. Also, it is important to analyze the shifts in the distances at which the maxima occur under different variations of the tissue's electrical parameters related to its total water content or physiopathological conditions. Finally, validating these results with in-vitro studies using models that emulate the skin's electrical properties and multilayer structure would be pertinent.

References

1. **Lo Presti, A., Montoya, N.A., Criscuolo, V., Khan, G., Khan, U., Vecchione, R., Falconi, C. (2023).** Fundamentals of Skin Bioimpedances. Advanced Materials, Vol. 35, No. 33, pp. 230–2127. DOI: 10.1002/adma.202302127.
2. **Grimnes, S., Martinsen, Ø.G. (2015).** Passive Tissue Electrical Properties. In **S. Grimnes et al. (Eds.),** Bioimpedance and Bioelectricity Basics, pp. 77–118. Elsevier. DOI: 10.1016/B978-0-12-4114 70-8.00004-0.
3. **Bora, D.J., Dasgupta, R. (2020).** Estimation of skin impedance models with experimental data and a proposed model for human skin impedance. IET Systems Biology, Vol. 14, No. 5, pp. 230–240. DOI: 10.1049/iet-syb.2020.0049.
4. **van Gerwen, P., Laureyn, W., Laureys, W., Huyberechts, G., Op De Beeck, M., Baert, K., Suls, J., Sansen, W., Jacobs, P., Hermans, L., Mertens, R. (1998).** Nanoscaled interdigitated electrode arrays for biochemical sensors. Sensors and Actuators B: Chemical, Vol. 49, No. 1–2, pp. 73–80. DOI: 10.1016/S0925-4005(98)00128-2.
5. **Herrera-Celis, J., Reyes-Betanzo, C., Orduna-Diaz, A. (2015).** Design of an interdigitated microelectrode biosensor using a SiC:H surface to capture E. coli. SBMicro 2015 - 30th Symposium on Microelectronics Technology and Devices. DOI: 10.1109/SBMicro.2015.729 8142.
6. **Noor, A.M., Zakaria, Z., Johari, S., Sabani, N., Wahab, Y., Manaf, A.A. (2021).** Numerical Simulation of Transdermal Iontophoretic Drug Delivery System. Journal of Physics: Conference Series, Vol. 2071, No. 1, 12–26. DOI: 10.1088/1742-6596/2071/1/012026.
7. **Italian National Research Council (2024).** Dielectric Properties of Body Tissues, from: http://niremf.ifac.cnr.it/tissprop/htmlclie/htmlclie. php.
8. **Zheng, H., Pu, Z., Wu, H., Li, C., Zhang, X., Li, D. (2023).** Reverse iontophoresis with the development of flexible electronics: A review. Biosensors and Bioelectronics, Vol. 223, pp. 115036. DOI: 10.1016/j.bios.2022.115036.
9. **Gill, H.S., Andrews, S.N., Sakthivel, S.K., Fedanov, A., Williams, I.R., Garber, D.A., Priddy, F.H., Yellin, S., Feinberg, M.B., Staprans, S.I., Prausnitz, M.R. (2009).** Selective removal of stratum corneum by microdermabrasion to increase skin permeability. European Journal of Pharmaceutical Sciences : Official Journal of the European Federation for Pharmaceutical Sciences, Vol. 38, No. 2, pp. 95–103. DOI: 10.1016/j.ejps.2009.06.004.
10. **Weigand, D.A., Gaylor, J.R. (1973).** Removal Of Stratum Corneum In Vivo: An Improvement On The Cellophane Tape Stripping Technique. Journal of Investigative Dermatology, Vol. 60, No. 2, pp. 84–87. DOI: 10.1111/1523-1747.ep12724 159.

Article received on 26/09/2024; accepted on 13/01/2025.
**Corresponding author is José Herrera-Celis.*